Parameters of dynamic polarization of As nuclei in silicon at low temperatures and strong magnetic fields

© M.B. Lifshits, V.A. Grabar, N.S. Averkiev

Ioffe Institute,
194021 St. Petersburg, Russia
E-mail: Averkiev@les.ioffe.ru

Received February 14, 2024
Revised February 27, 2024
Accepted February 28, 2024

The paper theoretically describes the solid effect in the Si : As structure in ESR conditions at low temperatures and in strong magnetic fields. A quantitative comparison of the results of calculating the dynamic polarization of As nuclei in silicon by the Overhauser mechanism and the solid effect with experimental data has been carried out. A good agreement between theory and experiment was demonstrated and the key parameter of the effects, the time of cross-relaxation transitions, was determined which turned out to be approximately 10 s for the As atom.

Keywords: ESR, solid effect, Overhauser effect, flip-flop transitions, silicon.

DOI: 10.61011/SC.2024.01.58116.6031

1. Introduction

Nuclear spins in nuclear magnetic resonance (NMR) conditions and electron spins in electron spin resonance (ESR) conditions are quantum objects that provide an opportunity to study the key magnetic properties of matter on a microscopic level. The efficiency of these methods may be increased if a significant nuclear polarization is achieved. The thermodynamic (equilibrium) polarization of nuclear spins in an external magnetic field is weak, and valuable signals in NMR thus have a relatively low intensity. However, a considerable dynamic non-equilibrium (although stationary) polarization of nuclear spins may be achieved in ESR conditions as the intensity of transitions with a change of the electron spin projection increases [1]. Dynamic nuclear polarization in [2,3] was established in ESR conditions for electrons localized at nitrogen vacancies in diamond. This provided an opportunity to amplify the NMR signal for certain defects in this material by an order of magnitude at low and room temperatures.

Dynamic nuclear polarization is made possible due to the hyperfine interaction between the spin of an electron localized at an impurity and the nuclear spin. Flip-flop transitions with simultaneous electron and nuclear spin flips are also needed. The duration of these transitions exceeds the time of electron spin relaxation, which preserves the nuclear spin projection, by several orders of magnitude; however, flip-flop transitions are the ones establishing an equilibrium distribution over nuclear spin projections in an external magnetic field. It is assumed that the time of nuclear spin relaxation (without including the interaction with a localized electron) in experiments is much longer than the times of electron spin relaxation and flip-flop transitions. Two major mechanisms of dynamic polarization in ESR conditions are distinguished. The first one (Overhauser effect) is implemented in excitation of allowed transitions with a change of the electron spin projection and preservation of the nuclear spin projection. The second mechanism (the so-called solid effect) is triggered under excitation of forbidden flip-flop transitions preserving the summary projection of an electron spin and a nuclear spin. Since dynamic nuclear polarization is significantly greater in magnitude than equilibrium nuclear polarization in an external magnetic field, equilibrium polarization is disregarded. The magnitude of dynamic nuclear polarization depends on ESR conditions. In moderate external fields and at helium temperatures (when the population difference between spin sublevels of an electron is not that large), the degree of orientation of nuclei is low and ESR line saturation measurements are needed to detect it. The pattern changes radically in strong magnetic fields and at low temperatures (when the populations of electron states with different spin projections differ by several orders of magnitude). The degree of nuclear polarization may reach 100% in this case under relatively weak pumping. These process conditions were examined in [4–7] for certain impurities in silicon.

The aim of the present study is to compare quantitatively the experimental data from [5] with the results of dynamic polarization calculations for the Overhauser effect [8] and calculated data on the solid effect (see below) for the purpose of estimating the time of flip-flop transitions and determining the mechanism of these transitions in Si : As. The time of flip-flop transitions was estimated in [5] under a simple assumption of exponential variation of the degree of nuclear polarization with time. However, it was demonstrated in [7,8] that the dependences of ESR signal magnitudes and the degree of dynamic nuclear polarization on pumping time cannot be characterized by a single exponential function and the exact time dependence of signal magnitudes are needed to obtain a correct estimate of transition times.

2. Dynamic polarization of As nuclei in the conditions of solid effect

An As impurity in Si induces a shallow donor level near each minimum of the conduction band. Due to

a strong valley-orbital interaction, the ground level is a valley-symmetric state that is doubly degenerate (with spin taken into account). The spin of an electron in silicon is 1/2, and the spin of an arsenic nucleus is 3/2. This implies that eight states with different projections of electron and nuclear spins onto the external magnetic field direction should be produced in an external magnetic field in the context of hyperfine interaction. The Hamiltonian characterizing this system is written as [5]

$$H = -g_e\mu_B S_z B_0 + g_n\mu_N I_z B_0 + A\mathbf{SI}. \qquad (1)$$

Here, $\mathbf{S}$ and $\mathbf{I}$ are the electron and nucleus spin operators, respectively, B_0 is the external magnetic field directed along z, g_e and g_n are the electron and nucleus g-factors, μ_B and μ_N are the Bohr and nuclear magnetons, $A = 198.35$ MHz is the hyperfine interaction constant for As^{75} atoms [5]. Term $g_n\mu_N I_z B_0$ describes the splitting of nuclear spin levels in the field and leads to the equilibrium polarization of nuclei, however, due to the small value of the nuclear Bohr magneton, this polarization is small in all fields and temperatures studied and therefore is neglected. $A\mathbf{SI}$ describes the hyperfine interaction between an electron spin and a nuclear spin. The value of A for all shallow impurities is significantly smaller than the splitting of electron spin levels in field B_0 and is accounted for by perturbation theory with respect to the dominant term: $g_E\mu_B S_z B_0$.

The energy positioning of levels is indicated in Figure 1 and is similar to level diagrams in [5,8]. The degree of dynamic polarization under pumping to forbidden flip-flop transitions P_{23}, P_{45}, P_{67} is calculated in the present study to determine the magnitude of the solid effect. The probabilities of transitions with the nuclear spin projection preserved are the same (vertical lines in Figure 1), and the probabilities of transitions between states with a change of the electron and nuclear spin projections depend on the nuclear spin projection. As was demonstrated in [5], the ratio of probabilities of transition $5 \to 4$ and transitions $3 \to 2$ and $7 \to 6$ is 4/3 (the ratio for relaxation times is an inverse one). A system of eight kinetic equations, which is similar to the system from [8], needs to be composed for calculation of the number of centers with different electron and nuclear spin projections:

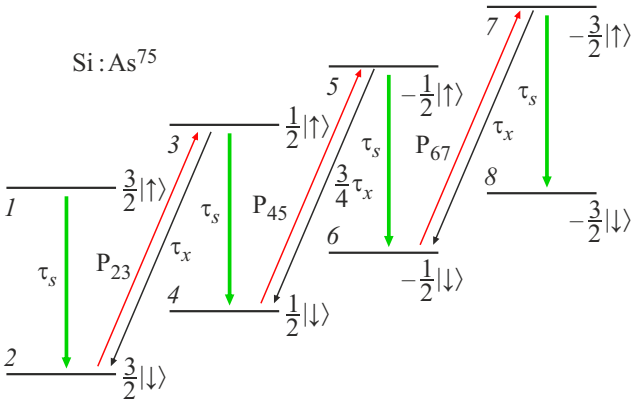

Figure 1. Diagram of spin sublevels of As^{75} in strong magnetic fields. Green and red lines denote transitions with an unchanged nuclear spin projection and cross transitions, respectively. (A color version of the figure is provided in the online version of the paper).

$$\begin{cases}
\dot{N}_1\tau_s = -\dfrac{N_1}{1+\mu} + \dfrac{\mu}{1+\mu}N_2, \\
\dot{N}_2\tau_s = \dfrac{N_1}{1+\mu} - \left[\dfrac{\mu}{1+\mu}\left(1+\dfrac{\tau_s}{\tau_x}\right) + P_{23}\tau_s\right]N_2 + \left[\dfrac{\tau_s}{\tau_x}\dfrac{1}{1+\mu} + P_{23}\tau_s\right]N_3, \\
\dot{N}_3\tau_s = \left[\dfrac{\mu}{1+\mu}\dfrac{\tau_s}{\tau_x} + P_{23}\tau_s\right]N_2 - \left[\dfrac{1+\dfrac{\tau_s}{\tau_x}}{1+\mu} + P_{23}\tau_s\right]N_3 + \dfrac{\mu}{1+\mu}N_4, \\
\dot{N}_4\tau_s = \dfrac{N_3}{1+\mu} - \left[\dfrac{\mu}{1+\mu}\left(1+\dfrac{4}{3}\dfrac{\tau_s}{\tau_x}\right) + P_{45}\tau_s\right]N_4 + \left[\dfrac{4}{3}\dfrac{\tau_s}{\tau_x}\dfrac{1}{1+\mu} + P_{45}\tau_s\right]N_5, \\
\dot{N}_5\tau_s = \left[\dfrac{\mu}{1+\mu}\dfrac{4}{3}\dfrac{\tau_s}{\tau_x} + P_{45}\tau_s\right]N_4 - \left[\dfrac{1+\dfrac{4}{3}\dfrac{\tau_s}{\tau_x}}{1+\mu} + P_{45}\tau_s\right]N_5 + \dfrac{\mu}{1+\mu}N_6, \\
\dot{N}_6\tau_s = \dfrac{N_5}{1+\mu} - \left[\dfrac{\mu\left(1+\dfrac{\tau_s}{\tau_x}\right)}{1+\mu} + P_{67}\tau_s\right]N_6 + \left[\dfrac{\tau_s}{\tau_x}\dfrac{1}{1+\mu} + P_{67}\tau_s\right]N_7, \\
\dot{N}_7\tau_s = \left[\dfrac{\mu}{1+\mu}\dfrac{\tau_s}{\tau_x} + P_{67}\tau_s\right]N_6 - \left[\dfrac{1+\dfrac{\tau_s}{\tau_x}}{1+\mu} + P_{67}\tau_s\right]N_7 + \dfrac{\mu}{1+\mu}N_8, \\
\dot{N}_8\tau_s = -\dfrac{\mu}{1+\mu}N_8 + \dfrac{N_7}{1+\mu}.
\end{cases} \qquad (2)$$

Here, N_i is the number of impurities in the i state, P_{lm} is the intensity of induced transitions for each line pair,

$$\mu = \exp(-g_e\mu_B B_0/kT),$$

where k is the Boltzmann constant and τ_s and τ_x are the relaxation times of spin and cross transitions $3 \to 2$ and $7 \to 8$, respectively. Equations (2) are written under the assumption that the sum of all N_i is a constant and equal to total number N of arsenic atoms. For $P_{ij} = 0$ and $\tau_x^{-1} = 0$, the system of equations is split into four independent subsystems, and equilibrium is established independently in each of them. Due to cross relaxation, thermodynamic equilibrium is established for states with different nuclear spin projections within $t \gg \tau_x \gg \tau_s$. Average nuclear spin $\mathscr{P}$ may be determined as the ratio of the number of impurities with a certain nuclear spin projection to the overall number of impurities in the system:

$$\mathscr{P} = \frac{\frac{3}{2}[N_1 + N_2 - N_7 - N_8] + \frac{1}{2}[N_3 + N_4 - N_5 - N_6]}{N}. \tag{3}$$

In stationary conditions $t \gg \tau_x \gg \tau_s$, the $\mathscr{P}_{lm}$ nuclear polarization expressions under pumping to one of the transitions take the form

$$\mathscr{P}_{23} = -\frac{3}{2}\frac{P_{23}\tau_x(1-\mu^2)}{4\mu + P_{23}\tau_x(\mu^2+4\mu+3)},$$

$$\mathscr{P}_{45} = -\frac{P_{45}\tau_x 3(1-\mu^2)}{8\mu + P_{45}\tau_x 3(1+\mu)^2},$$

$$\mathscr{P}_{67} = -\frac{3}{2}\frac{P_{67}\tau_x(1-\mu^2)}{4\mu + P_{67}\tau_x(3\mu^2+4\mu+1)}.$$

It is evident that the strongest nuclear polarization is achieved at $P_{lm}\tau_x \gg \mu$ and $\mu \ll 1$. These conditions are satisfied in strong magnetic fields when the populations of spin sublevels of an electron differ significantly. The magnitudes of nuclear polarization for each pumping line may be estimated as

$$\mathscr{P}_{23} = -\frac{3}{2}\frac{P_{23}\tau_x}{3P_{23}\tau_x + 4\mu} \approx -\frac{1}{2},$$

$$\mathscr{P}_{45} = -\frac{3P_{45}\tau_x}{3P_{45}\tau_x + 8\mu} \approx -1,$$

$$\mathscr{P}_{67} = -\frac{3}{2}\frac{P_{67}\tau_x}{P_{67}\tau_x + 4\mu} \approx -\frac{3}{2}.$$

In studying of the solid effect below, we calculate the dependence of the $\mathscr{P}_{23}$ nuclear polarization degree on time and the intensity of ESR lines with pumping P_{23}, since this case was investigated experimentally in [5].

In order to determine temporal variation $N_i(t)$ of populations, one needs to solve system (2) with account for initial conditions (depending on experimental conditions) and pumping to transition $2 \to 3$ that is initiated at time point $t = 0$. For the arbitrary values of the parameters, this is a difficult problem; however, when spin relaxation time τ_s of an electron is several orders of magnitude shorter than the cross-relaxation time τ_x, a solution of (2) may be obtained in an approximation linear in parameter τ_s/τ_x. We look for the solutions $N_i(t)$ in the form

$$N_i(t) = n_i \exp(-\lambda t/\tau_s)$$

and introduce the following notation:

$$\alpha = 1/(1+\mu), \quad \beta = \mu/(1+\mu).$$

Eigen values λ specify the relaxation times for populations N_i. Since system (2) consists of eight equations, it yields eight eigen values λ. The sum of all N_i is conserved; therefore, one of them should be equal to zero. To find these values, one needs to take into account the fact that the system at $\tau_s/\tau_x \to 0$ is split into four individual subsystems describing the equilibration of states with different electron and the same nuclear spin projections. If ratio τ_s/τ_x is finite but small, a stationary distribution between pairs of states with the same nuclear spin projections is achieved within a rather short time τ_s, and thermodynamic equilibrium between all eight levels is established within a time period specified by τ_x. At times longer than τ_s, the population of spin sublevels of an electron depends only on the population of the state with a specific nuclear spin projection. It is convenient to calculate n_i in new variables: $n_{12} = n_1 + n_2$, $Q_{12} = -\alpha n_1 + \beta n_2$, etc. In a linear approximation in τ_s/τ_x, Eqs. (2) for n_{ij} and Q_{ij} are then separated, and the following is obtained for n_{ij}:

$$\begin{cases} -\lambda\dfrac{\tau_x}{\tau_s}n_{12} + \alpha(\beta + P_{23}\tau_x)n_{12} - \beta(\alpha + P_{23}\tau_x)n_{34} = 0, \\ -\lambda\dfrac{\tau_x}{\tau_s}n_{34} - \alpha(\beta + P_{23}\tau_x)n_{12} \\ \qquad\qquad + \beta\left(\dfrac{7}{3}\alpha + P_{23}\tau_x\right)n_{34} - \dfrac{4}{3}\alpha\beta n_{56} = 0, \\ -\lambda\dfrac{\tau_x}{\tau_s}n_{56} + \dfrac{7}{3}\alpha\beta n_{56} - \dfrac{4}{3}\alpha\beta n_{34} - \alpha\beta n_{78} = 0, \\ -\lambda\dfrac{\tau_x}{\tau_s}n_{78} + \alpha\beta n_{78} - \alpha\beta n_{56} = 0. \end{cases} \tag{4}$$

The equations for Q_{ij} have a similar form in the same approximation, but their eigen values $\lambda = 1$ accurately to within a value on the order of τ_s/τ_x. System of equations (4) describes the variation of population of pairs of states with the same nuclear spin projections, and differences $N_{i+1} - N_i$ in population levels within each pair need to be determined for calculation of the time dependence of ESR signals. At times longer than τ_s, $Q_{ij} = 0$; this allows us to express $N_{i+1} - N_i$ in terms of $N_{ij} = N_i + N_j$. The dependences of relative ESR signal magnitudes for each level pair are defined as follows:

$$N_2 - N_1 = \alpha(1-\mu)N_{12}, \quad N_4 - N_3 = \alpha(1-\mu)N_{34},$$

$$N_6 - N_5 = \alpha(1-\mu)N_{56}, \quad N_8 - N_7 = \alpha(1-\mu)N_{78}.$$

It is convenient to calculate time dependences of N_{ij} by switching from algebraic system (4) back to a more intuitive form of differential kinetic equations:

$$\begin{cases} \dot{N}_{12}T_x + N_{12}(1 + P_{23}\tau_x/\beta) - N_{34}(1 + P_{23}\tau_x/\alpha) = 0, \\ \dot{N}_{34}T_x - N_{12}(1 + P_{23}\tau_x/\beta) \\ \qquad + N_{34}(7/3 + P_{23}\tau_x/\alpha) - 4/3N_{56} = 0, \\ \dot{N}_{56}T_x - 4/3N_{34} + 7/3N_{56} - N_{78} = 0, \\ \dot{N}_{78}T_x - N_{56} + N_{78} = 0, \end{cases} \tag{5}$$

where $T_x = \tau_x(1+\mu)^2/\mu$.

System (5) demonstrates that the time of transition to the stationary state differs from the introduced microscopic parameter τ_x and cannot be reduced to parameter T_x, since the coefficients at different N_{ij} depend on the $P_{23}\tau_x$ ratio. At low temperatures with $\mu \ll 1$, time T_x, which determines the process of equilibration in the nuclear subsystem under zero pumping, is significantly longer than the cross-relaxation time. This colossal time extension is attributable to the fact that the value of parameter $\lambda = 0$ is four times degenerate in initial system (2) at $\mu = 0$. This implies that the ratio of populations of sublevels in the stationary state should depend on the initial conditions and a nonzero equilibrium nuclear polarization is possible (if such a polarization was present at the initial time). At a finite μ, only one state with zero average nuclear spin is stationary. For the system to achieve it, transitions from electron spin-down states to a spin-up state are needed (see Figure 1 and system (2)). However, such a transition is proportional to the number of phonons, which is proportional to μ at low temperatures. Therefore, the system should reach an equilibrium state within a time proportional to τ_x/μ. The characteristic times of achieving to a stationary state decrease under pumping. At $\mu \ll 1$, ratio $P_{23}\tau_x/\mu$ is the parameter reducing the relaxation times. The solution of system (5) may be written as

$$N_{12}(t) = n_{34}^{(0)} \frac{1 + \dfrac{P_{23}\tau_x}{\alpha}}{1 + \dfrac{P_{23}\tau_x}{\beta}} + \sum_{k=1,2,3} n_{34}^{(k)} \frac{1 + \dfrac{P_{23}\tau_x}{\alpha}}{1 - t_k + \dfrac{P_{23}\tau_x}{\beta}} e^{-\lambda_k t},$$

$$N_{34}(t) = n_{34}^{(0)} + \sum_{k=1,2,3} n_{34}^{(k)} e^{-\lambda_k t},$$

$$N_{56}(t) = n_{34}^{(0)} + \sum_{k=1,2,3} n_{34}^{(k)} \frac{\dfrac{3}{4}t_k^2 - t_k\left(\dfrac{5}{2} + \dfrac{3}{4}\dfrac{P_{23}\tau_x}{\alpha\beta}\right) + 1 + \dfrac{P_{23}\tau_x}{\beta}}{1 - t_k + \dfrac{P_{23}\tau_x}{\beta}} e^{-\lambda_k t},$$

$$N_{78}(t) = n_{34}^{(0)} + \sum_{k=1,2,3} n_{34}^{(k)} \frac{\dfrac{3}{4}t_k^2 - t_k\left(\dfrac{5}{2} + \dfrac{3}{4}\dfrac{P_{23}\tau_x}{\alpha\beta}\right) + 1 + \dfrac{P_{23}\tau_x}{\beta}}{(1 - t_k)(1 - t_k + \dfrac{P_{23}\tau_x}{\beta})} e^{-\lambda_k t}, \tag{6}$$

where $\lambda_k = \alpha\beta t_k/\tau_x$ and t_k are the solutions of cubic equation

$$3t^3 - t^2\left(20 + \frac{3}{\alpha\beta}P_{23}\tau_x\right) + t\left(36 + \frac{2(5+2\alpha)}{\alpha\beta}P_{23}\tau_x\right) - \left(16 + \frac{4(1+2\alpha)}{\alpha\beta}P_{23}\tau_x\right) = 0,$$

constants $n_{34}^{(0)}$ and $n_{34}^{(k)}$ are determined from the initial conditions.

3. Comparison of theoretical and experimental results

Experimental studies of dynamic polarization of nuclear spins of As in Si in Overhauser effect and solid effect modes in strong magnetic fields at low temperatures were performed in [5]. The populations of electron sublevels with opposite electron spin projections differ significantly and parameter $\mu \ll 1$. Let us analyze the Overhauser effect first. We use the results from [8] with a coefficient of 4/3 in probabilities of cross-relaxation transitions (this difference was neglected in [8]). As was noted in [5,8], the highest stationary degree of dynamic polarization is observed under pumping of line 2. Therefore, this case is the one considered below. To observe the Overhauser effect, the authors of [5] first established the conditions in which nuclei were almost completely polarized in state $I_z = 1/2$; pumping to transition $4 \to 3$ was then switched on, and the dependence of ESR signals for $1 \to 2$ and $3 \to 4$ lines on pumping time was studied. Due to dynamic polarization, the $1 \to 2$ line intensity increased with time, while the $3 \to 4$ line intensity decreased to zero. Thus, nuclei were polarized preferentially in state $I_z = 3/2$.

Figure 2 presents the comparison of calculated (curves) and experimental [5] (squares, triangles, and circles) time dependences of populations and the degree of polarization of nuclei. Studying the Overhauser effect, we chose parameters τ_x and $P_{43}\tau_s$ such that the data from [5] were matched with (*a*) — the point of intersection between blue and red curves corresponding to transitions $1 \to 2$ and $3 \to 4$ (N_{12}, N_{34} and N_{56}); (*b*) — signal levels for transitions $1 \to 2$, $3 \to 4$, and $5 \to 6$ (N_{12}, N_{34} and N_{56}) in the stationary case (i. e., plateaus that they reach at times $t > \tau_x$); (*c*) — the tangent point of red and green curves corresponding to signals $3 \to 4$ and $5 \to 6$ (N_{34} and N_{56}). It turned out that the points of intersection between curves and the moment of plateauing shifted only insignificantly under small changes in parameter $P_{43}\tau_s$. The variation of

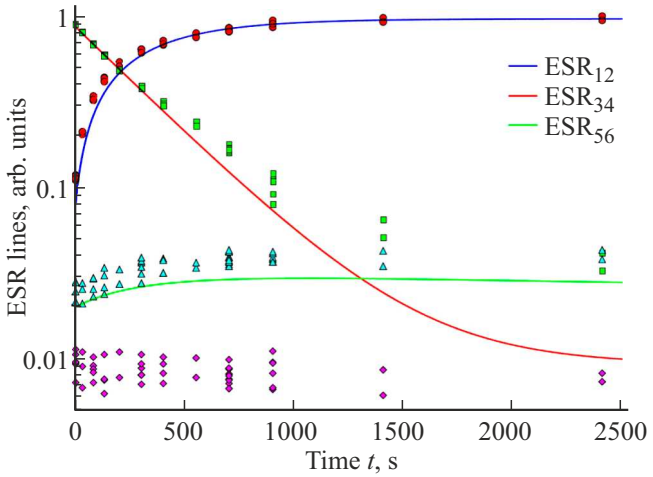

Figure 2. Time dependence of the ESR signal magnitude under $P_{43}\tau_s$ pumping for the Overhauser effect at $P_{43}\tau_s/\mu = 100$.

parameter τ_x affected only the overall slope of curves and, consequently, the moment of plateauing: the longer the time needed by a system to reach saturation is, the slower is the change of the curve position relative to the vertical axis. The cross-relaxation time determined in this comparison with experimental data was $\tau_x \approx 8.5$ s at $\mu \approx 2.36 \cdot 10^{-4}$. Note that the time of achieving to a stationary state depends on the pumping intensity; without pumping, thermodynamic equilibrium is established in more than 50 h.

When dynamic nuclear polarization under the solid effect was considered [5], pumping was performed between states 2 and 3. These transitions are less probable than those preserving the nuclear spin projection and more probable than transitions with a change in the summary projection of an electron spin and a nuclear spin. A sample was prepared in a polarized state with $I_z = 3/2$, and ESR signals for lines $1 \to 2$ and $3 \to 4$ were examined as functions of the time of pumping the $2 \to 3$ transition. In contrast to the case of the Overhauser effect with the $P_{43}\tau_s$ parameter specifying the pumping efficiency, parameter $P_{23}\tau_x$ was the governing one here.

Calculated (6) time dependences of ESR signals for the solid effect were compared with experimental ones [5] in much the same way as it was done for the Overhauser effect (see Figure 3), although an additional scale coefficient for the vertical axis, which was needed to take into account explicitly the conservation of total number of impurities N, had to be determined. It was taken into consideration that a clear transition of the system to a stationary state is not found in the figure from [5]; therefore, it was impossible to compare signals in the saturation mode. The variation of curves with changes in parameters τ_x and P_{23} was similar to that in the case of the Overhauser effect. Time $\tau_x \approx 9$ s was determined from the comparison of calculations with data for the solid effect. The time of achieving to a stationary state also depends on the pumping intensity in this case and reaches ~ 20 h at the chosen parameter values.

In addition to providing the experimental data presented above, the authors of [5] measured ESR signals of all four lines with successive pumping of transitions $8 \to 7$, $6 \to 5$, and $4 \to 3$ (for 2000 s each). The indicated time is much longer than the spin relaxation time of electrons, but is substantially shorter than the time of settling to a stationary state (according to the data for the solid effect, the latter time is 20 h). If the initial populations of all nuclear spin sublevels were the same and the ESR line intensities were equal, 2000 s of line pumping induced no

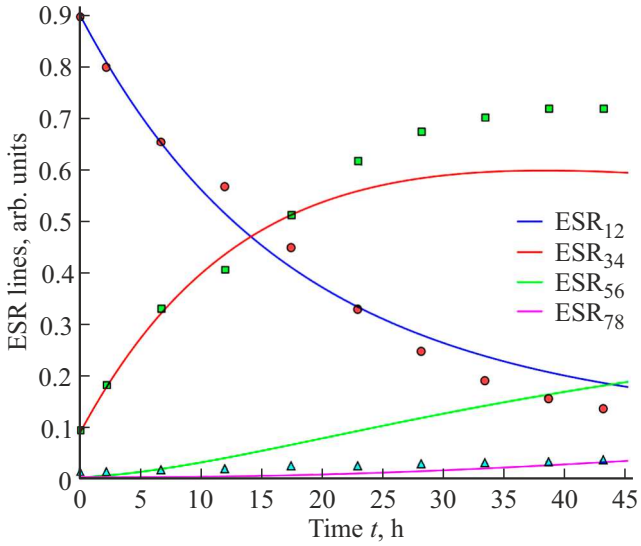

Figure 3. Time dependence of the ESR signal magnitude under P_{23} pumping for the solid effect, $P_{23}\tau_x/\mu = 4$. Solid curves represent the results of calculation by formulae (6); squares, circles, and triangles denote experimental data.

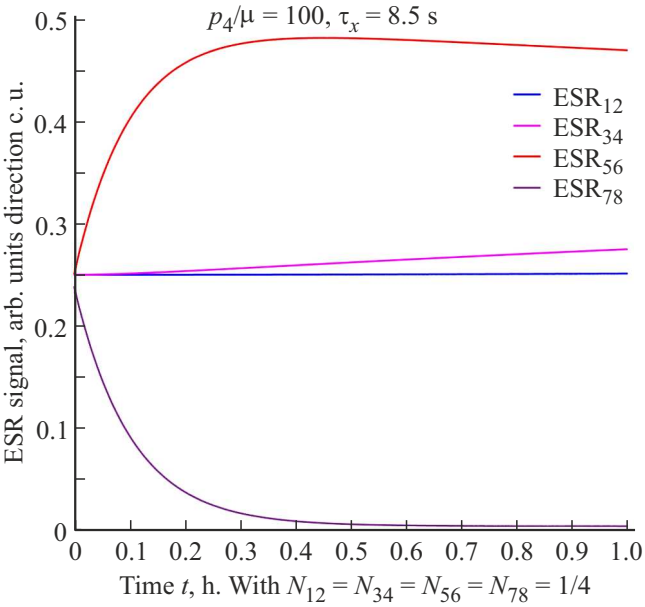

Figure 4. Time dependences of ESR signals for each line under pumping $P_{87}/\mu = 100$.

changes in the intensity of lines $5 \to 6$ and $3 \to 4$, while line $7 \to 8$ vanished almost completely and the $5 \to 6$ line intensity increased by a factor of 2. This implies that levels 7 and 8 were depopulated almost entirely and all electrons were redistributed between levels 5 and 6.

Figure 4 presents the results of our calculations of the temporal variation of line intensities performed with the use of parameters determined for the case under study. It is evident that the calculation results agree well with the data from [5], since the $5 \to 6$ line signal did indeed intensify within 2000 s, while line $7 \to 8$ vanished. The cases of pumping to lines $6 \to 5$ and $4 \to 3$ were also simulated, and a fine agreement with experimental data was achieved.

4. Conclusion

An in-depth comparison of theoretical and experimental data on the effect of dynamic polarization in Si:As was performed. The key parameter, cross-relaxation time τ_x, was determined. It turned out that this time is on the order of 10 s; its values derived from data on the Overhauser effect and the solid effect were almost equal. The values of critical parameters $P_{23}\tau_x = 1.1 \cdot 10^{-3}$ and $P_{43}\tau_s = 2.4 \cdot 10^{-2}$ were calculated. They are both slightly greater than μ, but remain much smaller than unity (i.e., ESR signal saturation is not reached). A τ_x value on the order of 1 s was also observed for Si:P [7], where the mixing of states with different nuclear spin projections by the hyperfine interaction was assumed to be the underlying mechanism of cross relaxation. Spin relaxation in Si for electrons localized at donors is governed by direct transitions with a change of the electron spin projection in interaction with long-wavelength acoustic phonons [9]. At low temperatures ($g_e\mu_B B_0/kT \gg 1$) τ_s is temperature-independent, but depends on the external magnetic field magnitude and, according to [9,10], assumes a value of 10^{-7}–10^{-8} s. Time τ_x is then also temperature-independent and is $(g_e\mu_B B_0/A)^2 \approx 10^6$ times greater than τ_s. This does no contradict the results reported here; however, the effect of dynamic polarization needs to be studied in various magnetic fields and at different temperatures in order to identify the mechanism of cross relaxation unambiguously.

Acknowledgments

The authors wish to thank L.S. Vlasenko for fruitful discussions and in-depth remarks regarding the experimental data.

Funding

This study was supported by the Russian Scientific Foundation, project No. 23-12-00205.

Conflict of interest

The authors declare that they have no conflict of interest.

References

[1] Y. Ishikawa, Y. Fujii, A. Fukuda, Y. Koizumi, T. Omija, T. Oida, H. Yamamori, A. Matsubara, S. Mitsudo, S. Lee, J. Järvinen, S. Vasiliev. Appl. Magnetic Res., **52**, 305 (2021).
[2] D.B. Bucher, D.R. Glenn, H. Park, M.D. Lukin, R.L. Walsworth. Phys. Rev. X, **10**, 021053 (2020).
[3] D. Shimon, K.A. Cantwell, L. Joseph, E.Q. Williams, Z. Peng, S. Takahashi, C. Ramanathan. J. Phys. Chem. C, **126**, 17777 (2022).
[4] J. Järvinen, D. Zvezdov, J. Ahokas, S. Sheludiakov, L. Lehtonen, S. Vasiliev, L. Vlasenko, Y. Ishikawa, Y. Fujii. Phys. Chem. Chem. Phys., **22**, 10227 (2020).
[5] J. Järvinen, J. Ahokas, S. Sheludiakov, O. Vainio, D. Zvezdov, L. Lehtonen, L. Vlasenko, S. Vasiliev. Appl. Magnetic Res., **48**, 473 (2017).
[6] J. Järvinen, J. Ahokas, S. Sheludyakov, O. Vainio, L. Lehtonen, S. Vasiliev, D. Zvezdov, Y. Fujii, S. Mitsudo, T. Mizusaki, M. Gwak, SangGap Lee, Soonchil Lee, L. Vlasenko. Phys. Rev. B, **90**, 214401 (2014).
[7] W. Knap, N. Averkiev, M. Lifshits, D. But. *Terahertz enhancement of dynamic nuclear polarization in semiconductors*. In: RJUSE-TeraTech2021 (2021).
[8] M.B. Lifshits, N.S. Averkiev. Solid State Commun., **371**, 115276 (2023).
[9] Hiroshi Hasegawa. Phys. Rev., **118**(6), 1523 (1960).
[10] Laura M. Roth. Phys. Rev., **118** (6), 1534 (1960).

Translated by D.Safin